Diethylene glycol ethers (111-90-0, 112-15-2, 112-59-4, 124-17-4, 6881-94-3)	US/ICCA	LP

（註）担当国の略号は AUS：オーストラリア、BE：ベルギー、CH：スイス、DE：ドイツ、FIN：フィンランド、FR：フランス、JP：日本、KO：韓国、NL：オランダ、SK：スロバキア共和国、US：米国である。ICCA は国際化学工業協会協議会による原案提出を示す。eu は、欧州連合でのリスク評価をもとにしたことを示す。合意結果において、FW は追加の調査研究作業が必要であることを、LP は現状では追加作業の必要がないことを示す。HH はヒトへの健康影響、ENV は環境影響について示し、－は合意に達しなかったことを示す。

化学生物総合管理　第 3 巻第 1 号（2007.6）　43-55 頁
連絡先：〒158-8501 東京都世田谷区上用賀 1-18-1　E-mail: ema@nihs.go.jp
受付日：2006 年 8 月 10 日　　受理日：2007 年 3 月 29 日

Available online at www.sciencedirect.com
ScienceDirect
Mutation Research 638 (2008) 48–55
Fundamental and Molecular Mechanisms of Mutagenesis
www.elsevier.com/locate/molmut
Community address: www.elsevier.com/locate/mutres

Mutagenic radioadaptation in a human lymphoblastoid cell line

Fumio Yatagai [a,*], Yukihiro Umebayashi [a], Masamitsu Honma [b], Kaoru Sugasawa [c], Yuko Takayama [a], Fumio Hanaoka [d]

[a] *Advanced Development and Support Center, The Institute of Physical and Chemical Research (RIKEN), Saitama 351-0198, Japan*
[b] *Division of Genetics and Mutagenesis, National Institute of Health Sciences, Tokyo 158-8501, Japan*
[c] *Genome Damage Response Research Unit, The Institute of Physical and Chemical Research (RIKEN), Saitama 351-0198, Japan*
[d] *Graduate Program, Frontiers in Biosciences, Osaka University, Osaka 565-0871, Japan*

Received 6 April 2007; received in revised form 15 August 2007; accepted 22 August 2007
Available online 1 September 2007

Abstract

We investigated the mutagenic radioadaptive response of human lymphoblastoid TK6 cells by pretreating them with a low dose (5 cGy) of X-rays followed by a high (2 Gy) dose 6 h later. Pretreatment reduced the 2-Gy-induced mutation frequency (MF) of the *thymidine kinase* (*TK*) gene (18.3×10^{-6}) to 62% of the original level (11.4×10^{-6}). A loss of heterozygosity (LOH) detection analysis applied to the isolated TK^- mutants revealed the mutational events as non-LOH (resulting mostly from a point mutation in the *TK* gene), hemizygous LOH (resulting from a chromosomal deletion), or homozygous LOH (resulting from homologous recombination (HR) between chromosomes). For non-LOH events, pretreatment decreased the frequency to 27% of the original level (from 7.1×10^{-6} to 1.9×10^{-6}). cDNAs prepared from the non-LOH mutants revealed that the decrease was due mainly to the repression of base substitutions. The frequency of hemizygous LOH events, however, was not significantly altered by pretreatment. Mapping analysis of chromosome 17 demonstrated that the distribution and the extent of hemizygous LOH events were also not significantly influenced by pretreatment. For homozygous LOH events, pretreatment reduced the frequency to 61% of the original level (from 5.1×10^{-6} to 3.1×10^{-6}), reflecting an enhancement in HR repair of DNA double-strand breaks. Our findings suggest that the radioadaptive response in TK6 cells follows mainly from mutations at the base-sequence level, not the chromosome level.

Keywords: Adaptive response; TK6 cells; LOH detection system

1. Introduction

An adaptive cellular response occurs when a mild stress applied before a challenging treatment with a DNA-damaging agent decreases the detrimental effects of the challenge. In radioadaptation, as it is usually defined, exposure to a low dose of ionizing radiation (IR) provides some protection against a high dose. Radioadaptation was first reported by Olivieri et al. [1], who showed that radiation delivered by labeling human lymphocytes with tritiated thymidine causes a decrease in the frequency of chromosomal aberrations induced by subsequent exposure to 15 Gy of IR. That discovery stimulated a series of studies in human lymphocytes and various mammalian cell lines (for review, see refs. [2,3]) and suggested that the adaptive response is an important defense mechanism, especially against low doses of IR. The molecular mechanisms involved, however, remain largely unknown [4–8], and cellular

* Corresponding author. Tel.: +81 48 467 9710; fax: +81 48 462 1426.
E-mail address: yatagai@postman.riken.go.jp (F. Yatagai).

0027-5107/$ – see front matter © 2007 Elsevier B.V. All rights reserved.
doi:10.1016/j.mrfmmm.2007.08.014

responses such as the bystander effect, genetic instability and hyper-radiosensitivity seem tightly related to the adaptive response in a specific low-dose region. One of the hot subjects in recent adaptive response studies is the expression of the genes involved in the mechanism [8–10]. Another is the relationship between the adaptive response and the bystander effect [11–15]. In mammalian cells, for example, bystander mutagenesis may be suppressed by an adaptive response [11].

Following the report by Olivieri et al., reduced induction of both micronuclei and sister chromatid exchanges was shown in Chinese hamster V79 cells pre-exposed to low doses of γ-rays or ^{3}H β-rays [16]. Subsequent studies reported similar radioadaptive responses, such as reduced mutation frequencies in human lymphocytes [17], mouse SR-1 cells [18] and human–hamster hybrid A_L cells [19], an altered mutation spectrum in human–hamster hybrid A_L cells [19], reduced micronucleus frequencies in human lymphocytes [5] and mouse embryo cells [20], and reduced deletions and rearrangements in human lymphoblast cells [21]. The mechanism underlying those radioadaptations may have been the induction of an efficient chromosome repair system by the priming radiation dose, and in fact, the efficiency of DNA double-strand break (DSB) repair in Chinese hamster V79 cells exposed to γ-rays is enhanced by a priming exposure of 5 cGy of γ-rays [22]. Furthermore, DSBs with either blunt or staggered ends, created by restriction enzymes, induce the adaptive response [3].

The human lymphoblastoid TK6 cell line, isolated by Skopek et al. [23], is heterozygous at the *thymidine kinase* (*TK*) locus. Honma's laboratory developed a loss of heterozygosity (LOH) detection system that can be used for molecular analysis of *TK* mutations as well as for detecting alterations at the chromosome level [24,25]. Using that methodology, we were able to detect IR effects at doses as low as 10 cGy [26–28]. Irradiation of TK6 cells with 10 cGy of X-rays clearly demonstrated radiation-specific types of LOH events or interstitial deletions in chromosome 17 [26]. We also observed more efficient induction of such events after 10 cGy irradiation with an accelerated carbon-ion (135 MeV/u) beam [27], and this was apparent in frozen cells exposed to the same carbon-ion beam [28]. These results strongly suggest that the interstitial deletions were the result of end-joining repair of IR-induced DSBs.

Because the radiation-sensitive LOH analysis system in TK6 cells is effective for detecting the fate of radiation-induced DNA double-strand breaks (DSBs), we use it here to see if the adaptive response could produce measurable changes in IR-induced genetic alterations. The results we obtained were not completely expected, but are interesting.

2. Materials and methods

2.1. Cell culture and adaptive treatment

The methodologies for the detection of *TK*-deficient mutants and the materials and methods used for cell culture and growth have been previously reported [26]. Briefly, TK6 cells were incubated in RPMI1640 medium supplemented with HAT to eliminate pre-existing TK^- deficient mutants. The cells were then resuspended in fresh normal medium, and 6 ml cell suspension was dispensed into 6-cm diameter Petri dishes. The cells were pretreated ("primed") with 2.5, 5 or 10 cGy of X-rays (250 kVp) at a rate of 10 cGy/min, and placed in a 5% CO_2 humidified incubator. The cell concentration was adjusted to 8×10^5 cells/ml at the end of the post-irradiation incubation period of 1.5, 3, 6, 9 or 12 h. The cells were then challenged with 2 Gy X-rays (250 kVp) at 1 Gy/min. Non-primed irradiated cells treated in the same manner as the primed cells served as controls.

2.2. Survival assay and TK mutation assay

To determine the surviving fraction of the challenged cells, we measured the plating efficiency (PE) immediately after irradiation using the limiting dilution method. For mutation expression, we incubated the cells with non-selecting RPMI1640 medium for about 60 h following the X-ray challenge. We measured the PE of incubated cells similarly, determining the *TK* mutation frequency. To select TK^- mutant clones, we seeded incubated cells into 96-well plates at 4×10^4 cells per well in RPMI1640 medium containing 4 μg/ml trifluorothymidine (TFT); we harvested the normally growing clones after 2 weeks and the slow growing clones after 4 weeks.

2.3. Determination of optimum irradiation conditions for mutagenic adaptation

To determine the optimum conditions for evoking the mutagenic radioadaptive-response, we tested the MF induced by 2 Gy at 0, 1.5, 3, 6, 9 and 12 h after a priming dose of 10 cGy, selected the optimum interval time, and then tested the MF induced by 2 Gy at that interval time after priming doses of 0, 2.5, 5 and 10 cGy.

2.4. LOH analysis of TK^- mutants

Fig. 1 illustrates how we classified TK^- mutants. We first determined *TK* LOH by PCR analysis of exons 4 and 7 [29]. If the PCR products of both were similar to those of the parental *TK* heterozygous cells, we classified the mutant

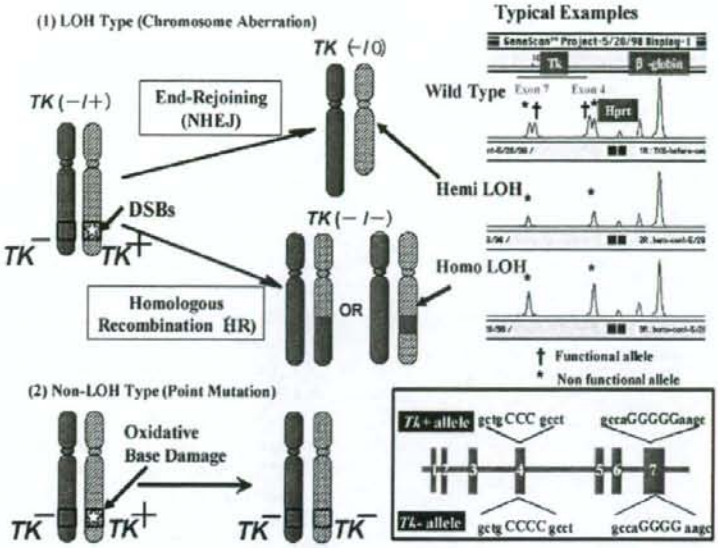

Fig. 1. LOH classifications of TK^- mutants. The first step in the genetic analysis of selected TK^- mutants was to judge whether there was a loss of *TK* heterozygosity (LOH). This was accomplished by PCR amplification of exons 4 and 7 regions of the *TK* locus. This step also distinguished between hemizygous LOH (loss of the functional *TK* allele) and homozygous LOH (replacement of the functional *TK* allele by a mutated TK^- allele (see ref. [29]).

as a "non-LOH" mutant. We used the same technique to distinguish between hemizygous LOH (in which the functional *TK* allele is lost) and homozygous LOH (in which the functional *TK* allele is replaced by TK^-). To determine the extent and size of the deleted or substituted portions of the chromosome involved, we analyzed 11 microsatellite regions (D17S588, D17S1784, D17S785, D17S789, D17S802, D17S807, D17S928, D17S932, D17S1299, D17S1566 and THRA) on chromosome 17 using multiple PCR reactions as described previously [29]. The fine structure of the recovered TK^- LOH mutations was determined by chromosome mapping analysis.

2.5. Base sequencing of non-LOH mutants

For a precise analysis of non-LOH mutants, we extracted RNA using Isogen (Nippon Gene, Japan), and obtained cDNA using a First-Strand cDNA Synthesis Kit, Amersham, USA). Following PCR amplification, the purified 807-bp fragments were sequenced by Takara Bio (Japan). The primers 5′-AGAGTACTCGGGTTCGTGAA-3′ and 5′-GCAGCATGCAGGGCAGCGTG-3′ (forward and reverse, respectively) were used for cDNA synthesis, PCR amplification and base sequencing [30]. To prevent the overestimation of mutational events, we counted identical mutations originating from a single irradiated dish as a single event.

Table 1a
TK mutation frequency (MF) at various time intervals between priming and challenging X-ray exposures (priming dose, 10 cGy; challenging dose, 2 Gy)

Time interval (h)	0	1.5	3	6	9	12
TK MF ($\times 10^{-6}$)	19.8	18.1	14.4	13.5	17.8	19.7

3. Results

3.1. Optimum conditions for mutagenic adaptation

For inducing an adaptive response to X-ray irradiation, the optimum interval between a 10-cGy priming dose and a 2-Gy challenging dose was 6 h (Table 1a), and the optimum priming dose 6 h prior to a 2-Gy challenging dose was 5 cGy (Table 1b). We therefore decided to characterize the induced *TK* mutants by repeating

Table 1b
TK mutation frequency at various priming X-ray doses (challenging dose, 2 Gy; interval between 2 exposures, 6 h)

Priming X-ray dose (cGy)	0	2.5	5	10
TK MF ($\times 10^{-6}$)	13.3	15.8	4.5	6.3

Table 2
Surviving fractions of primed and non-primed TK6 cells following challenge exposure to 2 Gy X-rays

Experiment	Surviving fraction	
	Non-primed cells	Primed cells (5 cGy)
I	0.043	0.047
II	0.047	0.070
III	0.049	0.040
Mean ± S.D.	0.046 ± 0.0031*	0.052 ± 0.016*

* $P = 0.58$; t-test.

Table 3
TK mutation frequency in primed and non-primed TK6 cells following challenge exposure to 2 Gy X-rays

Experiment	*TK* mutation frequencies ($\times 10^{-6}$)	
	Non-primed cells	Primed cells (5 cGy)
I	13.3	4.5
II	13.3	10.5
III-a	20.4	15.1
III-b	21.0	15.6
Mean ± S.D.	18.3 ± 4.3*	11.4 ± 5.1*

Experiments III-a and III-b were carried out concurrently with survival assay III, but they were independent mutation assays.
* $P = 0.020$; t-test.

our mutation experiments under those conditions (5 cGy followed 6 h later with 2 Gy).

3.2. Survival assay and TK mutation assay

Table 2 shows the surviving fraction, expressed as PE (2 Gy X-ray irradiated cells)/PE (unirradiated cells) of primed and unprimed cells immediately after the 2-Gy challenge exposure. Irradiation with the priming dose of 5 cGy did not influence the PE of unchallenged cells (data not shown). The effect of priming on survival after 2 Gy X-ray irradiation was 1.1 (0.052/0.046; $P = 0.58$, t-test). Thus, priming did not significantly affect survival after the challenge exposure.

On the other hand, priming did affect the *TK* MF induced by the challenge. Data from 4 independent experiments showed that priming reduced the MF to 62% of the unprimed MF ($P = 0.020$, t-test) (Table 3).

3.3. LOH analysis of TK^- mutants

Table 4 shows the distributions of LOH classes among the isolated TK^- mutants as determined by PCR analysis. We isolated non- and "small" LOH mutants (see Sections 3.4 & 3.5) as normal growth mutants in the first selection, except for a few cases. We isolated the remaining LOH mutants as slow growth mutants in the second selection. We estimated the pre-exposure effect from the proportion of each mutational event as follows: (i) 7.1×10^{-6} to 1.9×10^{-6} reduction in corresponding MF of non-LOH events, (ii) 6.4×10^{-6} to 6.1×10^{-6} change in corresponding MF of hemizygous LOH events and (iii) 5.1×10^{-6} to 3.1×10^{-6} reduction in corresponding MF of homozygous LOH events. Thus, the MF of a non-LOH event in primed cells was reduced to 27% of the non-primed MF. The induction of hemizygous events, on the other hand, was barely influenced by priming. As far as homozygous events go, their corresponding MF was reduced to 61% of the original level, which was similar to level of reduction in total MF (62%).

3.4. Analysis of LOH tracts on chromosome 17

Fig. 2 shows the deleted or replaced regions of chromosome 17 in each LOH mutant. Mutants reflected both type 1 and type 2 LOH events. Type 1 defines a terminal event; that is, the deleted or exchanged chromosome segment extends to the telomere marker (D17S928). Type 2 defines an interstitial deletion; the altered segment does not reach the telomere marker.

In the present study, most hemizygous LOH mutations, which are considered to be the result of DSB non-homologous end-joining (NHEJ) repair, reflected

Table 4
Distribution of mutational classes among the isolated *TK* mutants

Mutational class	Number of identified mutants (Exp. I, II, III-a, III-b) [MF $\times 10^{-6}$]	
	Non-primed cells	Primed cells (5 cGy)
Non-LOH	18 (5, 4, 6, 3) [7.1]	8 (1, 3, 2, 2) [1.9]
LOH		
Hemizygous	15 (3, 3, 7, 2) [6.0]	27 (8, 7[a], 5, 7) [6.4]
Homozygous	13 (3, 4, 3, 3) [5.1]	13 (2, 3, 5, 3) [3.1]
Total	46 (11, 11, 16, 8) [18.3]	48 (11, 13, 12, 12) [11.4]

[a] One of the seven mutants was a mixed hemizygous/homozygous type.

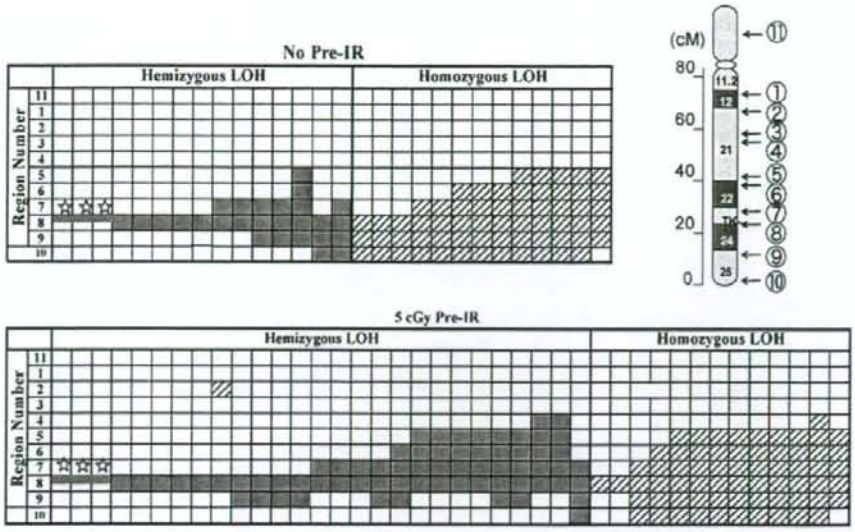

Fig. 2. Chromosome mapping of the LOH mutants. We analyzed the LOH mutants selected after a 2 Gy of challenging X-ray irradiation to determine the extent of the deleted or exchanged portions of the chromosome. The upper panel shows the profiles of 28 LOH mutants selected from non-primed cells, and the lower panel shows the profiles of 40 LOH mutants selected from cells primed with 5 cGy of X-rays. Each column represents a single LOH mutant. The rows represent regions of chromosome 17 diagrammed in the upper right insert. Shaded squares represent deleted regions and hatched squares represent exchanged regions (see text). The region numbers refer to the 11 microsatellite regions: (1) D17S588; (2) D17S1784; (3) D17S785; (4) D17S789; (5) D17S802; (6) D17S807; (7) D17S928; (8) D17S932; (9) D17S1299; (10) D17S1566; (11) THRA (see ref. [29]). The star symbol represents a "small" type 2 hemizygous event in which the deletion is restricted to *TK* locus.

type 2 events in both the non-primed (13 of 15 mutants) and primed (26 of 27 mutants) groups. Small type 2 deletions – those restricted to the *TK* locus (Fig. 2) – were infrequent in both groups (3 of 15 mutants in non-primed cells and 3 of 27 in primed cells). Similarly, the proportion of large deletion mutants (expanding to the region beyond region 8, Fig. 2) was also similar in the primed (18 of 27 mutants) and non-primed (7 of 15 mutants) groups. Homozygous LOH events, on the other hand, which are considered to be the result of homologous recombination (HR) repair of DSBs, were primarily identified as type 1 events in both primed (10 of 13) and non-primed (12 of 13) groups. Interestingly, small homozygous LOH events (where only a single region was replaced, Fig. 2) were recovered from the primed cells (2 of 13 (3 0f 14)), but not from the non-primed cells (0 of 13).

3.5. Analysis of non-LOH-mutants

We detected many types of alterations in the non-LOH mutant cDNAs (Table 5). The proportion of single base-substitutions among all the mutations identified as this class was 1/8 (13%) in the primed cells, and this value was clearly lower than 7/18 (87%) in the unprimed cells. G and C bases were targeted in base substitution mutations, except for a single case of an A to T transversion (Table 5). Most (4/5) of the double-base changes consisted of a single base deletion (causing a frameshift) and a base substitution, except for a single case of a GC to TA double transversion in a radioadapted mutant. It is difficult to estimate the effect of priming on the induction of the double-base change events from the limited number of cells involved. Similar difficulties were also found in the other mutational events in this class such as triple-base changes, multiple-base changes and exon skipping. In addition, the proportion of abnormal transcription events (both functional and non-functional *TK* alleles are equally transcribed) was also similar in the radioadapted (1/8, 13%) and the non-adapted (3/18, 17%) group, although its origin was not identified.

4. Discussion

The radioadaptation conditions used in this study (5 cGy of priming X-rays followed in 6 h by 2 Gy of challenging X-rays) were similar to those used in other studies [4,6,11,12,14,16]. The *TK* mutation frequency

Table 5
Nature of the isolated non-LOH mutants

Type of mutation		Number of identified mutants	
Specific changes	[Position: exon]	Non-primed exposure	Primed (5 cGy) pre-X-ray
Single base substitutions		7	1
G → A (Gly → Glu)	[56:1]	3	0
C → T (Gln → Stop)	[64:1]	1	0
C → A (Ser → Stop)	[89:2]	1	0
A → T (Ser → Cys)	[97:2]	1	0
G → C (Leu → Phe)	[108:2]	0	1
G → A (Glu → Lys)	[430:6]	1	0
Double base changes		3	2
G → A (Gly → Glu)/Del. C	[56:1/676:7]	1	0
G → C (Leu → Phe)/Del. A	[108:2/686:7]	0	1
Add. C/Del. G	[232:4/641:7]	1	0
GC → TA (Leu Asp → Leu Asn)	[372 and 373:5]	0	1
G → A (Glu → Lys)/Del. G	[430:6/447:6]	1	0
Triple base changes		0	1
Del. G/C → T (Ile → Ile)/C → T (Leu → Leu)	[92:1/288:4/561:7]	0	1
Multiple base changes		1	1
CC → AT (Thr Gln → Thr Stop)/G → A (Gln → Gln)/G → A (Gln → Gln)/Add. C/Del. G	[51 and 52:1/66:1/667:7/232:4/641:7]	0	1
Base changes at 20 sites		1	0
Exon skipping, abnormal splicing and deletion		3	2
Del. of a part of exon 1 (48 bases)	[161–209: 1]	1	1
Abnormal splicing of intron (between exons 1 and 2)		1	0
Skipping of exon 3 (Del. 111 bases)	[99–203: 3]	1	0
Skipping of exon 5 (Del. 90 bases)	[304–393: 5]	0	1
Abnormal transcription		3	1
Both functional and non-functional alleles are equally transcribed			
Unidentified		1	0
Total		18	8

we observed after the challenge X-rays (18.3×10^{-6}) was reduced by the 5-cGy priming exposure to about 62% of the non-primed level (11.4×10^{-6}). Taking into consideration the *TK* spontaneous mutation frequency observed in our recent study (3.0×10^{-6}) [32], the increase in MF induced by 2 Gy of X-rays was reduced from 6.1-fold to 3.8-fold.

We originally planned this study to determine whether radioadaptation would alter the characteristics of X-ray-induced LOH events. X-ray-induced interstitial deletions are likely to be the result of NHEJ repair of DSBs, and this type of mutation was the one we recovered most frequently after 2 Gy X-ray irradiation in our previous study [24]. We also found that carbon-ion beam irradiation induced interstitial deletions more efficiently than the same dose of X-rays [26,27], which we interpreted as the result of a higher occurrence of inaccurately repaired DSBs. In the present study, however, we found that the frequency of hemizygous LOH mutations, as well as their size and the distribution of deleted regions on chromosome 17, was similar for radioadapted and non-adapted cells. Those results are not consistent with reports suggesting that enhanced repair of DSBs reduces chromosomal alterations [21,22]. An entire genome assay might lead to results similar to the ones in those reports, but our observations were restricted to the *TK* locus on chromosome 17.

On the other hand, we observed a decrease in the induction of homozygous LOH events in the primed cells, which suggests that priming enhanced the HR repair of DSBs. We recently constructed a model system to follow the fate of a single DSB introduced by the restriction enzyme I-sceI at a specific site in the *TK* gene in TK6 cells [31]. In preliminary exper-

iments, low dose/low-dose rate γ-irradiation (30 mGy at 1.2 mGy/h) did not significantly affect end joining (EJ) repair of this specific DSB, but it enhanced the efficiency of HR repair by about 50% (unpublished data). The small homozygous LOH events we observed in the primed cells in the present study (3/14) might reflect this enhanced HR, but we must examine whether the adaptive response was really involved because we also recovered small homozygous LOH mutants after the low-dose/low-dose rate γ-ray exposures [32]. The decrease in the frequency of single-base substitutions that we observed in primed cells (1/48) versus non-primed cells (7/46) (Tables 4 and 5) is rarely influenced by counting base substitutions accompanied by single base deletions (which would result in 2/48 for primed cells and 9/46 for non-primed cells), so the most likely mechanism for the reduced induction of non-LOH mutants was suppression of base substitutions.

One of the possible targets for radioadaptation is oxidative base damage. In fact, down-regulation of the human *CDC16* gene that occurs after oxidative stress causes more rapid and efficient repair in adapted (2 cGy pre-irradiated) human lymphoblastoid cells challenged with 4 Gy irradiation [6]. On the other hand, oxidative base excision repair enzymes, including DNA glycosylases, hOGG1 and hNth1, are reportedly not up-regulated at the post-transcriptional level in γ-ray-primed TK6 cells [33]. Since DNA glycosylase can suppress base substitution, we need to examine whether radioadaptation enhances the enzyme's activity under the present condition. Alternatively, base substitution activity might not accurately reflect DNA glycosylase activity because attempted base excision repair of IR damage by the enzyme can lead to lethal and mutagenic DSBs [34].

A variety of untargeted effects may contribute to the short- and long-term fate of a cell exposed to IR [35]. An example is the possible involvement of a "radioadaptive bystander" effect in human lung fibroblasts [36]. The reduction of radiosensitivity in cells with a wild type *p53* gene by a radiation-induced, nitric oxide (NO)-mediated bystander effects may be a manifestation of the radioadaptive response [37,38]. This possibility is supported by the finding that the NO-induced apoptosis observed in lymphoblastoid and fibroblast cells depends on the phosphorylation and activation of p53 [39]. However, it is still unclear whether the NO-mediated pathway also contributes to the mutagenic adaptation. The de novo protein synthesis is required for expression of adaptive responses [22,40], and gene expression studies are improving our understanding of the molecular mechanisms underlying the radioadaptive response [9,10,40,41]. Our laboratory is also focusing on the molecular mechanisms involved in radioadaptation, especially the expression of genes involved in DNA base and nucleotide excision repair.

Acknowledgements

This study was partially supported by the Budget for Nuclear Research of the Ministry of Education, Culture, Sports, Science and Technology, and was reviewed by the Atomic Energy Commission of Japan. We thank Dr. Miriam Bloom (SciWrite Biomedical Writing & Editing Services) for professional editing.

References

[1] G. Olivieri, Y. Bodycote, S. Wolf, Adaptive response of human lymphocytes to low concentrations of radioactive thymidine, Science 223 (1984) 594–597.
[2] S. Wolf, Aspects of the adaptive response to very low doses of radiation and other agents, Mutat. Res. 358 (1996) 135–142.
[3] S. Wolf, The adaptive response in radiobiology: evolving insights and implications, Environ. Health Pesrpect. 106 (1998) 277–283.
[4] O. Rigaud, E. Moustacchi, Radioadaptation for gene mutation and the possible molecular mechanisms of the adaptive response, Mutat. Res. 358 (1996) 127–134.
[5] M. Wojewodska, M. Kruzewski, K. Iwanenko, I. Szumiel, Effects of signal transduction in adapted lymphocytes: micronuclei frequency and DNA repair, Int. J. Radiat. Biol. 71 (1997) 245–252.
[6] P.-K. Zhou, O. Rigaud, Down-regulation of the human *CDC16* gene after exposure to ionizing radiation: a possible role in the radioadaptive response, Radiat. Res. 155 (2001) 43–49.
[7] M.S. Sasaki, Y. Ejima, A. Tachibana, T. Yamada, K. Ishizaki, T. Shimizu, T. Nomura, DNA damage response pathway in radioadaptive response, Mutat. Res. 504 (2002) 101–118.
[8] I. Szumiel, Adaptive responses: stimulated DNA repair or decreased damage fixation? Int. J. Radiat. Biol. 81 (2005) 233–241.
[9] M.A. Coleman, E. Yin, L.E. Peterson, D. Nelson, K. Sorensen, J.D. Tucker, A.J. Wyrobeck, Low-dose irradiation alters the transcript profiles of human lymphoblastoid cells inducing genes associated with radioadaptive response, Radiat. Res. 164 (2005) 369–382.
[10] H.P. Wang, X.H. Long, Z.Z. Sun, O. Rigaud, Q.Z. Xu, Y.C. Huang, J.L. Sui, B. Bai, P.K. Zhou, Identification of differentially transcribed genes in human lymphoblastoid cells irradiated with 0.5 Gy of γ-ray and the involvement of low dose radiation inducible CHD6 gene in cell proliferation and radiosensitivity, Int. J. Radiat. Biol. 82 (2006) 181–190.
[11] S.G. Swant, G. Randers-Pehrson, N.F. Metting, E.J. Hall, Adaptive response and the bystander effect induced by radiation in C3H 10T1/2 cells in culture, Radiat. Res. 156 (2001) 177–180.
[12] H.N. Zhou, G. Randers-Pehrson, C.R. Geard, D.J. Brenner, E.J. Hall, T.K. Hei, Interaction between radiation-induced adaptive response and bystander mutagenesis in mammalian cells, Radiat. Res. 160 (2003) 512–516.
[13] W.M. Bonner, Thresholds, bystander effect, and adaptive response, Proc. Natl. Acad. Sci. U.S.A. 100 (2003) 4973–4975.
[14] S.A. Mitchell, S.A. Marino, D.J. Brenner, E.J. Hall, Bystander effect and adaptive response in C3H 10T(1/2) cells, Int. J. Radiat. Biol. 80 (2004) 465–472.

[15] T.K. Hei, R. Persaud, H. Zhou, M. Suzuki, Genotoxicity in the eyes of bystander cells, Mutat. Res. 568 (2004) 111–120.
[16] T. Ikushima, Chromosomal response to ionizing radiation reminiscent of an adaptive response in cultured Chinese hamster cells, Mutat. Res. 180 (1987) 215–221.
[17] B.J.S. Sanderson, A.A. Morely, Exposure of human lymphocytes to ionizing radiation reduces mutagenicity by subsequent radiation, Mutat. Res. 164 (1986) 151–347.
[18] P.K. Zhou, X.Y. Liu, W.Z. Sun, Y.P. Zhang, Y.P.K. Wei, Cultured mouse SR-1 cells exposed to low-dose of γ-rays become less susceptible to the induction of mutations by radiation as well as bleomycin, Mutagenesis 8 (1993) 109–111.
[19] A.M. Ueno, D.B. Vannais, S.L. Gustafson, J.C. Wong, C.A. Waldren, A low adaptive dose of gamma-rays reduced the number and altered the spectrum of S1 mutants in human hamster hybrid cells, Mutat. Res. 358 (1996) 161–169.
[20] E.I. Azzam, G.P. Raaphorst, R.E. Mitchel, Radiation-induced adaptive response for protection against micronucleus formation and neoplastic transformation in C3H 10T1/2 mouse embryo cells, Radiat. Res. 138 (1994) S28–S31.
[21] O. Rigaud, D. Papadopoulo, E. Moustacchi, Decreased deletion mutation in radioadapted human lymphoblast, Radiat. Res. 133 (1993) 94–101.
[22] T. Ikushima, H. Aritomi, J. Morisita, Radioadaptive response: efficient repair of radiation-induced DNA damage in adapted cells, Mutat. Res. 358 (1996) 193–198.
[23] T.R. Skopek, H.L. Liber, B.W. Penman, W.G. Thilly, Isolation of a human lymphoblastoid line heterozygous at the thymidine kinase locus: possibility for a rapid human cell mutation assay, Biochem. Biophys. Res. Commun. 84 (1978) 411–416.
[24] M. Honma, M. Hayashi, T. Sofuni, Cytotoxic and mutagenic responses to X-rays and chemical mutagens in normal and p53-mutated human lymphoblastoid cell, Mutat. Res. 374 (1996) 89–98.
[25] M. Honma, L.S. Zhang, M. Hayashi, K. Takeshita, Y. Nakagawa, N. Tanaka, T. Sofuni, Illegitimate recombination leading to allelic loss and unbalanced translocation in p53-mutated human lymphoblastoid cells, Mol. Cell. Biol. 17 (1997) 4774–4781.
[26] S. Morimoto, T. Kato, M. Honma, M. Hayashi, F. Hanaoka, F. Yatagai, Detection of genetic alterations induced by low-dose X rays: analysis of loss of heterozygosity for *TK* mutation in human lymphoblastoid cells, Radiat. Res. 157 (2002) 533–538.
[27] S. Morimoto, M. Honma, F. Yatagai, Sensitive detection of LOH events in a human cell line after C-ion beam exposure, J. Radiat. Res. 43 (Suppl.) (2002) S163–S167.
[28] Y. Umebayashi, M. Honma, T. Abe, H. Ryuto, H. Suzuki, T. Shimazu, N. Ishioka, M. Iwaki, F. Yatagai, Mutation induction after low-dose carbon-ion beam irradiation of frozen human cultured cells, Biol. Sci. Space 19 (2005) 237–241.
[29] F. Yatagai, S. Morimoto, T. Kato, M. Honma, Further characterization of loss of heterozygosity enhanced by p53 abrogation in human lymphoblastoid TK6 cells: disappearance of endpoint hotspots, Mutat. Res. 560 (2004) 133–145.
[30] A.J. Grosvsky, B.N. Walter, C.R. Giver, DNA-sequence specificity of mutations at the human thymidine kinase locus, Mutat. Res. 289 (1993) 231–243.
[31] M. Honma, M. Izumi, M. Sakuraba, S. Tadokoro, H. Sakamoto, W. Wang, F. Yatagai, M. Hayashi, Deletion, rearrangement, and gene conversion; genetic consequences of chromosomal double-strand breaks in human cells, Environ. Mol. Mutagen. 42 (2003) 288–298.
[32] Y. Umebayashi, M. Honma, M. Suzuki, H. Suzuki, T. Shimazu, N. Ishioka, M. Iwaki, F. Yatagai, Mutation induction in cultured human cells after low-dose and low-dose-rate γ-ray irradiation: detection by LOH analysis, J. Radiat. Res. 48 (2006) 7–11.
[33] M. Inoue, G.-P. Shen, M.A. Chaudhry, H. Galick, J.O. Blaisdell, S.S. Wallace, Expression of the oxidative base excision repair enzymes is not induced in TK6 human lymphoblastoid cells after low doses of ionizing radiation, Radiat. Res. 161 (2004) 409–417.
[34] N. Yang, H. Galick, S.S. Wallace, Attempted base excision repair of ionizing radiation damage in human lymphoblastoid cells produces lethal and mutagenic double-strand breaks, DNA Repair 3 (2004) 1323–1334.
[35] P.J. Coates, S.A. Lorimore, E.G. Wright, Damaging and protective cell signaling in the untargeted effects of ionizing radiation, Mutat. Res. 568 (2004) 5–20.
[36] R. Iyer, B.E. Lehnert, Low-dose, low-LET ionizing radiation-induced radioadaptation and associated early responses in unirradiated cells, Mutat. Res. 503 (2002) 1–9.
[37] H. Matsumoto, A. Takahashi, T. Ohnishi, Radiation-induced adaptive and bystander effects, Biol. Sci. Space 18 (2004) 247–254.
[38] H. Matsumoto, A. Takahashi, T. Ohnishi, Nitric oxide radicals choreograph a radioadaptive response, Cancer Res. 67 (2007) 8574–8579.
[39] L.M. McLaughlin, B. Demple, Nitric oxide-induced apoptosis in lymphoblastoid and fibroblast cells dependent on the phosphorylation and activation of p53, Cancer Res. 65 (2005) 6097–6104.
[40] J.H. Yongblom, J.K. Wiencke, S. Wolf, Inhibition of the adaptive response of human lymphocytes to very low doses of ionizing radiation by the protein synthesis inhibitor cyclobeximide, Mutat. Res. 227 (1989) 257–261.
[41] L.-H. Ding, M. Shingyoji, F. Chen, J.-J. Hwang, S. Burma, C. Lee, J.-F. Chen, D.J. Chen, Gene expression profiles of normal human fibroblasts after exposure to ionizing radiation: a comparative study of low and high doses, Radiat. Res. 164 (2005) 17–26.

doi:10.1016/j.jmb.2008.01.033 J. Mol. Biol. (2008) 377, 1015–1023

JMB

Available online at www.sciencedirect.com

ScienceDirect

ELSEVIER

Miscoding Properties of 2′-Deoxyinosine, a Nitric Oxide-Derived DNA Adduct, during Translesion Synthesis Catalyzed by Human DNA Polymerases

Manabu Yasui[1]*, Emi Suenaga[2], Naoki Koyama[1], Chikahide Masutani[3], Fumio Hanaoka[3], Petr Gruz[1], Shinya Shibutani[4], Takehiko Nohmi[1], Makoto Hayashi[1] and Masamitsu Honma[1]

[1]*Division of Genetics and Mutagenesis, National Institute of Health Sciences, 1-18-1 Kamiyoga, Setagaya, Tokyo 158-8501, Japan*

[2]*Division of Pharmacognosy, Phytochemistry and Narcotics, National Institute of Health Sciences, 1-18-1 Kamiyoga, Setagaya, Tokyo 158-8501, Japan*

[3]*Cellular Biology Laboratory, Graduate School of Frontier Biosciences, Osaka University, 1-3 Yamada-oka, Suita, Osaka 565-0871, Japan*

[4]*Department of Pharmacological Sciences, State University of New York at Stony Brook, Stony Brook, NY 11794-8651, USA*

Received 26 November 2007; received in revised form 10 January 2008; accepted 14 January 2008
Available online 18 January 2008

Edited by J. Karn

Chronic inflammation involving constant generation of nitric oxide (•NO) by macrophages has been recognized as a factor related to carcinogenesis. At the site of inflammation, nitrosatively deaminated DNA adducts such as 2′-deoxyinosine (dI) and 2′-deoxyxanthosine are primarily formed by •NO and may be associated with the development of cancer. In this study, we explored the miscoding properties of the dI lesion generated by Y-family DNA polymerases (pols) using a new fluorescent method for analyzing translesion synthesis. An oligodeoxynucleotide containing a single dI lesion was used as a template in primer extension reaction catalyzed by human DNA pols to explore the miscoding potential of the dI adduct. Primer extension reaction catalyzed by pol α was slightly retarded prior to the dI adduct site; most of the primers were extended past the lesion. Pol η and pol κΔC (a truncated form of pol κ) readily bypassed the dI lesion. The fully extended products were analyzed by using two-phased PAGE to quantify the miscoding frequency and specificity occurring at the lesion site. All pols, that is, pol α, pol η, and pol κΔC, promoted preferential incorporation of 2′-deoxycytidine monophosphate (dCMP), the wrong base, opposite the dI lesion. Surprisingly, no incorporation of 2′-deoxythymidine monophosphate, the correct base, was observed opposite the lesion. Steady-state kinetic studies with pol α, pol η, and pol κΔC indicated that dCMP was preferentially incorporated opposite the dI lesion. These pols bypassed the lesion by incorporating dCMP opposite the lesion and extended past the lesion. These relative bypass frequencies past the dC:dI pair were at least 3 orders of magnitude higher than those for the dT:dI pair. Thus, the dI adduct is a highly miscoding lesion capable of generating A→G transition. This •NO-induced adduct may play an important role in initiating inflammation-driven carcinogenesis.

Keywords: inflammation; nitric oxide; DNA adduct; translesion synthesis; nonradioactive analysis

*Corresponding author. E-mail address: m-yasui@nihs.go.jp

Abbreviations used: •NO, nitric oxide; dI, 2′-deoxyinosine; dX, 2′-deoxyxanthosine; dA, 2′-deoxyadenosine; 8-OxodG, 8-oxo-2′-deoxyguanosine; dNTP, 2′-deoxynucleoside triphosphate; Alexa546, Alexa Fluor 546 dye; pol α, human DNA polymerase α; pol η, human DNA polymerase η; pol κ, human DNA polymerase κ; pol κΔC, a truncated form of pol κ; F_{ins}, frequency of insertion; F_{ext}, frequency of extension; 8-NO_2-dG, 8-nitro-2′-deoxyguanosine; dCMP, 2′-deoxycytidine monophosphate; dTMP, 2′-deoxythymidine monophosphate; dTTP, 2′-deoxythymidine triphosphate; dCTP, 2′-deoxycytidine triphosphate; dGTP, 2′-deoxyguanosine triphosphate; Cy3, Cyanin 3; endo V, endonuclease V.

0022-2836/$ – see front matter

Introduction

Chronic inflammation involving constant generation of nitric oxide ($^{\bullet}NO$) by macrophages has been recognized as a factor related to carcinogenesis.[1-3] $^{\bullet}NO$ can attack neighboring epithelial and stromal cells by damaging the DNA, altering their genome stability. There are two possible major pathways for the $^{\bullet}NO$ reaction (Fig. 1). One pathway involves the combination of $^{\bullet}NO$ and superoxide with the formation of highly toxic peroxynitrite ($ONOO^-$). Spontaneous hydrolysis of peroxynitrite under physiological conditions generates secondary radical species ($^{\bullet}NO_2$, $^{\bullet}OH$, and $CO_3^{\bullet-}$) that induce oxidation and nitration of diverse DNA adducts[4,5] such as 8-oxo-2'-deoxyguanosine (8-OxodG) and 8-nitro-2'-deoxyguanosine (8-NO_2-dG).[6,7] A second involves nitrosative deamination of DNA base by $^{\bullet}NO$ via formation of several nitrosating agents, which predominantly exist as nitrous anhydride (N_2O_3) at physiological pH.[8] The DNA base products by nitrosative deamination mainly involve conversion of adenine to hypoxanthine [2'-deoxyinosine (dI)] (Fig. 2), guanine to xanthine [2'-deoxyxanthosine (dX)], and cytosine to uracil.[9-12]

The spectrum of nitrosative DNA adducts in N_2O_3-treated plasmid DNA was composed of approximately 2% dC–dG cross-links, 4–6% abasic sites, and 25–35% each of dI, dX, and 2'-deoxyuracyl.[12,13] Moreover, dI and dX, as well as lipid peroxidated adducts, were increased in the cellular DNA of tissues from the $^{\bullet}NO$-overproducing SJL mouse model of inflammation.[14] The increased production of $^{\bullet}NO$ was associated with an increased mutation frequency.[15] When human TK6 cells were exposed to $^{\bullet}NO$, the increase in mutation rates observed at hypoxanthineguanine phosphoribosyltransferase and thymidine kinase gene loci correlated with the 40-fold increase of dI and dX more than did that of the controls in the cellular DNA.[10] Thus, the dI adduct is one of the major $^{\bullet}NO$-derived DNA lesions and may contribute to the burden of carcinogenesis in inflammation tissue.

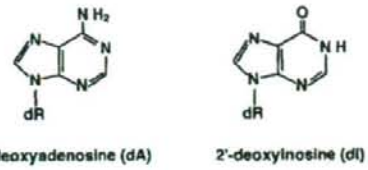

Fig. 2. Structures of dA and dI adducts.

Site-specifically dI-modified oligodeoxynucleotides have been used as DNA templates for investigating the miscoding events using only mouse pol α and rat pol β.[16] The previous report showed that rat pol β inserted only 2'-deoxycytidine monophosphate (dCMP) opposite the dI lesion and that mouse pol α tended to incorporate dCMP and 2'-deoxythymidine monophosphate (dTMP) opposite the lesion. However, the miscoding events were investigated with the detection of mismatched base pairs by loss of a restriction enzyme recognition site. No quantitative analysis, therefore, has been performed for determination of miscoding events generated by dI.

Human DNA pol η[17] and pol κ[18,19] that are associated with translesion synthesis past a variety of DNA lesions[20,21] were examined. We have here explored the miscoding properties of the dI lesion that occurred during DNA replication catalyzed by

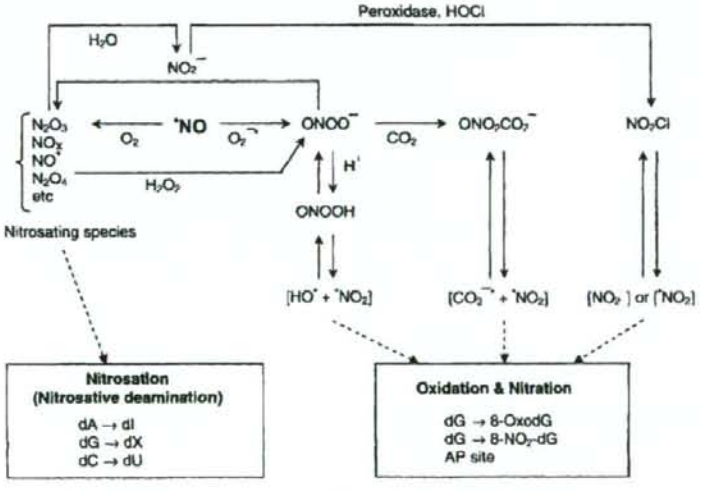

Fig. 1. Possible pathways for the formation of $^{\bullet}NO$-induced DNA adducts.

human DNA pols. In addition, instead of using radioisotope, we have developed a new fluorescent technique for analyzing translesion synthesis and quantifying the miscoding specificity and frequency using two-phased PAGE (Fig. 3).[22,23] Relative bypass frequencies past the dI lesion were also determined by steady-state kinetic studies.[24,25]

Results

Primer extension reactions catalyzed by human DNA pols on dI-modified DNA template

Using unmodified and dI-modified 38-mer templates, we conducted primer extension reactions in the presence of four 2'-deoxynucleoside triphosphates (dNTPs) and varying amounts of pol α, pol η, or pol κΔC (Fig. 4). Primer extension occurred rapidly on unmodified templates to form fully extended products. With the dI-modified template, primer extension catalyzed by pol α was slightly retarded one base before the lesion (see arrowhead in Fig. 4). However, when pol η or pol κΔC was used, primer extension resulted in fully extended products. No blockage was detected at the dI adduct site. When the amounts of pols were increased, products representing more than 32-mer bases long were produced on the unmodified and dI-modified templates. Blunt-end addition to the fully extended product (33–34-mers) was observed, as reported earlier for *Escherichia coli* and mammalian DNA pols.[26,27]

Miscoding frequencies and specificities of the dI adduct

Translesion synthesis catalyzed by pol α, pol η, or pol κΔC was conducted in the presence of all four dNTPs. The fully extended products (approximately 28–34-mers) past the unmodified or modified adducts were recovered, digested by EcoRI, and subjected to two-phased PAGE for quantitative analysis of base substitutions and deletions as described in Materials and Methods (Fig. 3). A standard mixture of six Alexa Fluor 546 dye (Alexa546)-labeled oligodeoxynucleotides containing dC, dA, dG, or dT opposite the lesion or one- and two-base deletions can be resolved by this method (Fig. 5). The percentage of 2'-deoxynucleoside monophosphate incorporation was normalized to the amount of the starting primer. When an unmodified dA template was used, expected incorporation of dTMP, the correct base, was observed opposite dA (Fig. 5). As indicated by the arrowhead in Fig. 5b, small amounts of unknown products were detected. When pol α was used with a template containing dI, dCMP (83.3% of the starting primers) was exclusively incorporated opposite the lesion. Similarly, pol η and pol κΔC promoted preferential incorporation of dCMP (55.0% and 74.7%, respectively) opposite the lesion. No deletions were detected. Surprisingly, no incorporation of dTMP, the correct base, was detected opposite the dI adduct with all pols, that is, pol α, pol η, and pol κΔC.

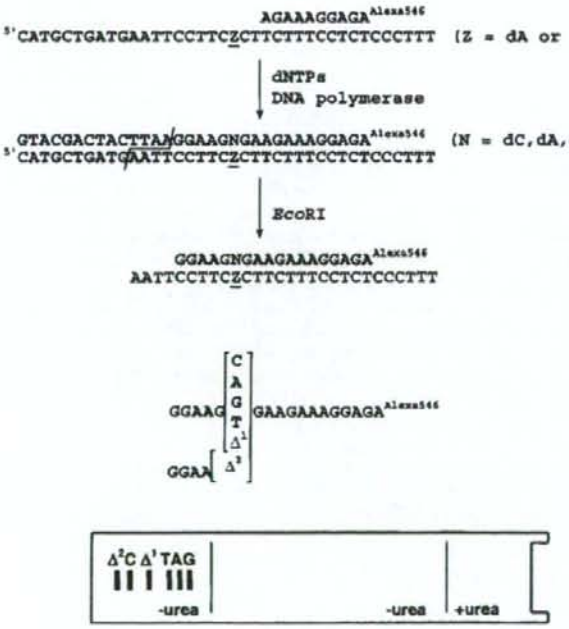

Fig. 3. Diagram of the fluorescent two-phased PAGE to determine miscoding specificity of DNA adducts. Unmodified and dI-modified 38-mer templates are annealed to either an Alexa546-labeled 10-mer primer or an Alexa546-labeled 12-mer primer. Primer extension reactions catalyzed by DNA pol α, pol η, or pol κΔC were conducted in the presence of four dNTPs. Fully extended products formed during DNA synthesis were recovered from the polyacrylamide gel (30 × 40 × 0.05 cm), annealed with a complementary 38-mer, cleaved with EcoRI, and subjected to a two-phased PAGE (20 × 65 × 0.05 cm), as described in Materials and Methods. To determine miscoding specificity, mobilities of the reaction products were compared with those of 18-mer standards containing dC, dA, dG, or dT opposite the lesion and one-base (Δ^1) or two-base (Δ^2) deletions.

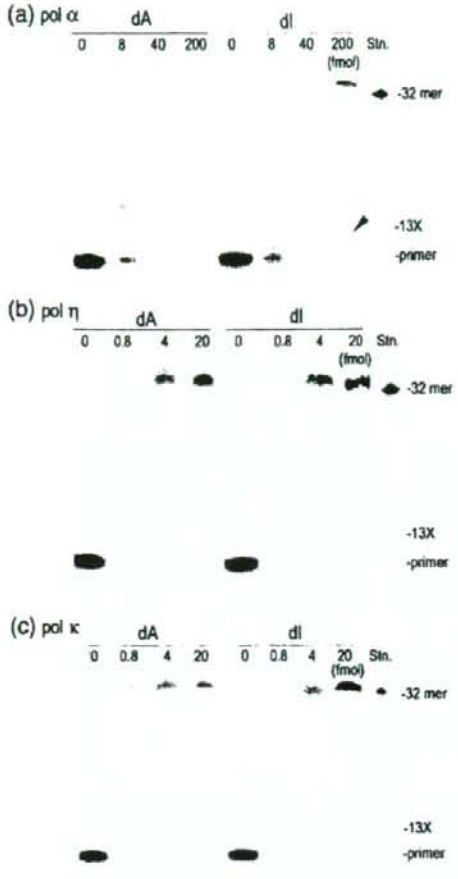

Fig. 4. Primer extension reactions catalyzed by pol α, pol η, or pol κΔC on dI-modified DNA template. Using unmodified or dI-modified 38-mer templates primed with an Alexa546-labeled 10-mer, we performed primer extension reactions at 25 °C for 30 min in a buffer containing four dNTPs (100 μM each) and varying amounts of (a) pol α (0, 8, 40, and 200 fmol), (b) pol η, or (c) pol κΔC (0, 0.8, 4, and 20 fmol), as described in Materials and Methods. The whole amount of the reaction mixture was subjected to 20% denaturing PAGE (30 × 40 × 0.05 cm). An Alexa546-labeled 32-mer (5'AGAGGAAAGTAGCGAAGGAATTCATCAGCATG) was used as a marker of fully extended product. 13X represents the adducted position

Kinetic studies on dI-modified templates

Steady-state kinetic studies were performed using pol α, pol η, and pol κΔC to determine the frequency of dNTP incorporation (F_{ins}) opposite the dI lesion and chain extension (F_{ext}) from the primer terminus using the same sequence context that was used for the two-phased PAGE assay (Table 1). With pol α, the F_{ins} value for deoxythymidine triphosphate (dTTP) (1.21×10^{-2}), the correct base, opposite the dI was 59 times lower than that for 2'-deoxycytidine triphosphate (dCTP) (0.718). The relative bypass frequency ($F_{ins} \times F_{ext}$) past the dC:dI pair was approximately 2100 times higher than that for the dT:dI pair. F_{ins} and F_{ext} values for dA:dI and dG:dI were not detectable. When pol η was used, the F_{ins} value for dCTP (0.551), the wrong base, opposite the dI was 27 times higher than that for dTTP (2.07×10^{-2}) and was 17 and 75 times higher than that for 2'-deoxyadenosine triphosphate and 2'-deoxyguanosine triphosphate (dGTP), respectively. The F_{ext} value for the dC:dI pair was also higher than that for other 2'-deoxynucleoside monophosphates paired with dI. As a result, the $F_{ins} \times F_{ext}$ value past dC:dI was at least 3 orders of magnitude higher than that past other pairs. Similarly, with pol κ, $F_{ins} \times F_{ext}$ past dC:dI was much higher than that for other base pairs. F_{ins} and F_{ext} values for dTTP were 119 and 55 times lower than that for dCTP, respectively. Thus, all pols, that is, pol α, pol η, and pol κΔC, exclusively promote misincorporation of dCMP opposite the dI lesion during translesion synthesis, since $F_{ins} \times F_{ext}$ values of other dNTPs were considerably lower that that for dCTP, the wrong base.

Discussion

Primer extension reactions catalyzed by DNA pols are a powerful method to explore translesion synthesis past DNA adducts and their accompanying kinetic parameters of nucleotide insertion and extension. A ^{32}P-labeled oligodeoxynucleotide at the 5'-terminus is widely employed in such analyses; however, the handling of hazardous radioisotopes is intricate for use and waste disposal. Indeed, use of radioisotopes is restricted in many countries including Japan. As an alternative to ^{32}P, we used fluorescent dyes, Alexa546 and Cyanin 3 (Cy3), to label the 5'-terminus of the oligodeoxynucleotide used as primers and standard markers. The detection limits of Alexa546- and Cy3-labeled primers were approximately 120 and 240 times lower than that of the ^{32}P-labeled primer, respectively. However, when Alexa546-labeled primers (500 fmol) were annealed with DNA template (750 fmol) and the assays of primer extension and kinetic studies were carried out in this work, the resultant data were quantitative and reproducible (Figs. 6 and 7). Alexa546 exhibits a more sensitive and photostable fluorescence than Cy3. Moreover, even under repeated thawing and melting, an Alexa546-labeled oligomer stored at −20 °C was not degraded for at least 6 months. Using this method, we determined the miscoding frequency and specificity of 8-OxodG, which is known to generate predominantly 2'-deoxyadenosine monophosphate misincorporation at the lesion site. The results obtained from Alexa546 labeling were consistent with that from ^{32}P labeling (data not shown). Thus, Alexa546 was applicable to two-phased PAGE. Therefore, we have used this fluorescent method to explore translesion synthesis past dI adducts and its miscoding specificity and frequency using two-phased PAGE.

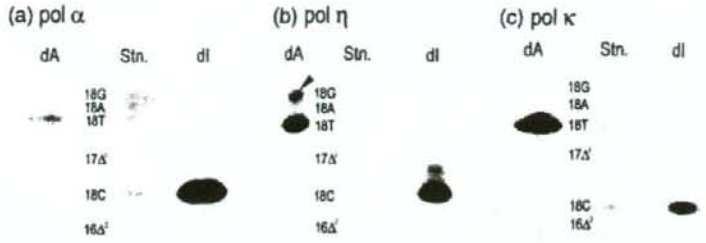

Fig. 5. Miscoding specificities of the dI lesion in reactions catalyzed by pol α, pol η, or pol κΔC. Using unmodified and dI-modified 38-mer templates primed with an Alexa546-labeled 12-mer, we conducted primer extension reactions at 25 °C for 30 min in a buffer containing four dNTPs (100 μM each) and either pol α (200 fmol for unmodified and dI-modified templates), pol κΔC, or pol η (20 fmol for unmodified and dI-modified templates), as described in Materials and Methods. The extended reaction products (>26 bases long) produced on the unmodified and dI-modified templates were extracted following PAGE. The recovered oligodeoxynucleotides were annealed to an unmodified 38-mer and cleaved with EcoRI restriction enzyme, as described in Materials and Methods. The entire product from the unmodified and dI-modified templates was subjected to two-phased PAGE (20 × 65 × 0.05 cm). Mobilities of reaction products were compared with those of 18-mer standards (Fig. 3) containing dC, dA, dG, or dT opposite the lesion and one-base (Δ^1) or two-base (Δ^2) deletions.

The mutation spectrum induced by ·NO has been investigated in a variety of experimental systems. ·NO gas showed mutagenicity in TK6 cells[10] and caused predominantly A:T→G:C transitions in plasmids replicated in cultured human and *E. coli* cells[28,29] and C→T transitions in a bacterial system.[9] Moreover, ·NO-releasing compounds exclusively resulted in G:C→A:T transitions in pSP189 plasmids propagated in human cells.[30] Using similar ·NO-releasing compounds, ONOO⁻ caused G:C→T:A and G:C→C:G transversions with the same experimental system.[31,32] Thus, based on the information obtained from these previous reports, the mutation spectrum by ·NO has not been extensively determined yet.[33] In our previous studies, the miscoding frequencies and specificities of dX, 8-NO_2-dG, and 8-OxodG lesions were quantitatively determined by two-phased PAGE. As a result, 8-NO_2-dG[34] and 8-OxodG[17,35] are miscoding lesions generating primarily G→T transversions (~20% and ~38%, respectively), while the miscoding spectrum of the dX adduct[36] exclusively shows G→A transitions (~50%), which differs from that of 8-NO_2-dG and 8-OxodG. This indicates that each DNA adduct has a unique miscoding specificity and frequency. The mutation spectrum by ·NO can be hardly determined due to the presence of diverse

Table 1. Kinetic parameters for nucleotide insertion and chain extension reactions catalyzed by human DNA pol α, pol η, and pol κΔC

		Insertion dNTP			Extension dGTP			
		5'-GAAGAAAGGAGA^{Alexa546} / 3'CCTTCZCTTCTTTCCTCTCCCTTT			5'-NGAAGAAAGGAGA^{Alexa546} / 3'CCTTCZCTTCTTTCCTCTCCCTTT			
	N:Z	K_m (μM)[a]	V_{max} (% min^{-1})[a]	F_{ins}	K_m (μM)[a]	V_{max} (% min^{-1})[a]	F_{ext}	$F_{ins} \times F_{ext}$
Pol α	T:A	0.56±0.03	0.53±0.02	1.0	0.31±0.14	0.31±0.03	1.0	1.0
	C:Z	0.73±0.26	0.47±0.03	0.718	0.48±0.09	0.25±0.01	0.679	0.487
	A:Z	N.D.	N.D.	N.D.	N.D.	N.D.	N.D.	N.D.
	G:Z	N.D.	N.D.	N.D.	N.D.	N.D.	N.D.	N.D.
	T:Z	9.74±1.60	0.11±0.07	1.21×10^{-2}	7.09±1.30	10.1±0.65	1.92×10^{-2}	2.32×10^{-4}
Pol η	T:A	0.65±0.17	5.37±0.26	21.0	0.69±0.13	7.49±0.11	1.0	1.0
	C:Z	1.74±0.58	7.79±0.48	0.351	0.96±0.18	8.44±0.25	0.809	0.446
	A:Z	4.87±1.22	1.28±0.03	3.18×10^{-2}	6.63±0.76	2.66±0.08	3.66×10^{-2}	1.16×10^{-2}
	G:Z	16.1±1.03	1.00±0.01	7.30×10^{-3}	11.6±4.23	1.14±0.11	9.40×10^{-3}	6.86×10^{-3}
	T:Z	7.00±1.97	1.19±0.03	2.07×10^{-2}	6.76±0.41	4.99±0.02	6.72×10^{-2}	1.39×10^{-2}
Pol κΔC	T:A	1.43±0.38	11.1±0.47	1.0	0.55±0.07	13.9±0.54	1.0	1.0
	C:Z	1.36±0.40	10.3±0.41	0.987	0.79±0.76	13.1±0.12	0.651	0.642
	A:Z	13.5±4.30	1.10±0.05	9.23×10^{-3}	10.7±2.43	2.17±0.07	8.13×10^{-3}	7.50×10^{-3}
	G:Z	84.0±15.4	0.76±0.30	1.12×10^{-3}	12.8±2.25	0.51±0.05	1.57×10^{-3}	1.75×10^{-3}
	T:Z	23.5±6.93	1.30±0.11	8.26×10^{-3}	5.28±0.37	1.59±0.03	1.18×10^{-2}	9.74×10^{-5}

Kinetics of nucleotide insertion and chain extension reactions were determined as described in Materials and Methods. Frequencies of nucleotide insertion (f_{ins}) and chain extension (f_{ext}) were estimated by the following equation: $f = (V_{max}/K_{m(adjusted\ for\ dNTP)})_{pol}/(V_{max}/K_{m(adjusted\ for\ dNTP)})_{N:Z}$. Z = dA or dI lesion.

N.D., not detectable.

[a] Data are expressed as mean ± SD obtained from three independent experiments.

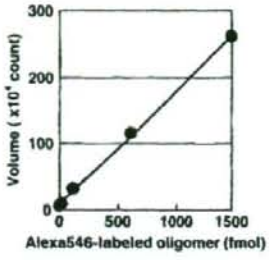

Fig. 6. Calibration curve using fluorescent oligomers labeled by Alexa546. Varying amounts of Alexa546-labeled oligomer were subjected to 20% denaturing PAGE. The volume of bands was quantitatively measured by using Molecular Imager FX Pro and Quantity One software (Bio-Rad) to find a linear range in the fluorescent analysis.

DNA adducts caused by ·NO-involved species (Fig. 1) and its miscoding variety.[17,34,35] Therefore, the quantitative miscoding properties of each ·NO-derived DNA adduct must be required to explore its roles in the inflammation-driven carcinogenesis.

The miscoding specificity of dI was determined by using an *in vitro* experimental system that can quantify base substitutions and deletions formed during replication in the presence of four dNTPs. Pol α, pol η, and pol κΔC incorporated dCMP (83.3%, 55.0%, and 74.7%, respectively) preferentially opposite the dI lesion rather than dTMP, the correct base (Fig. 5). Kamiya *et al.* reported earlier that mouse pol α inserted dCMP and dTMP, the correct base, opposite the dI lesion.[16] In contrast, human pol α promoted direct incorporation of dCMP only (Fig. 5). These indicate that the pols promote miscoding by incorporating dCMP opposite the dI lesion during DNA synthesis. Thus, dI is a highly miscoding lesion, generating A→G transitions in human cells. Steady-state kinetic studies supported these results. When pol α, pol η, and pol κΔC were used, $F_{ins} \times F_{ext}$ values for dC:dI pairs were 2100, 320, and 6600 times higher than those for dT:dI pairs, respectively (Table 1). Therefore, the kinetic results were consistent with that observed using two-phased PAGE analysis. Taken together, both analyses showed that human

Fig. 7. Typical image of PAGE for kinetic studies performed by Alexa546 labeling. Using unmodified or dI-modified 38-mer templates (750 fmol) primed with an Alexa546-labeled 12-mer (500 fmol), we conducted primer extension reactions at 25 °C for 2 min in a buffer containing pol κΔC (1 fmol) and either dTTP (0.25–25 μM for unmodified templates) or dCTP (0.25–25 μM for dI-modified templates), as described in Materials and Methods. The whole amount of the reaction mixture was subjected to 20% denaturing PAGE (30 × 40 × 0.05 cm).

DNA pols miscode at dI lesions by exclusively incorporating dCMP. The miscoding specificity was consistent with that observed in *E. coli*,[9] mammalian cells,[10,37] and mice exposed to ·NO.[15]

To compare the relative bypass frequency of dI, dX, and 8-NO_2-dG by pol α, pol η, and pol κΔC, these adducts were embedded in a similar sequence context[34,36] (Table 2). With pol α, the $F_{ins} \times F_{ext}$ ratio for the dC:dI/dT:dI pairs was 2100. This number was remarkably higher than that for the dT:dX/dC:dX (ratio = 1.5) or dA:8-NO_2-dG/dC:8-NO_2-dG (ratio = 0.01) pairs. Similar results were observed with pol η and pol κΔC. The ratios of $F_{ins} \times F_{ext}$ past dI were 2 orders of magnitude higher than those of dX and 8-NO_2-dG. Thus, dI adducts promote a higher miscoding potential (A→G transitions) than those of dX or 8-NO_2-dG. However, the highly mutagenic dI lesions did not show serious mutation frequency[9,10] even though they were predominantly paired with the wrong base, dCMP. Endonuclease V (endo V) has shown to be a dI-specific endonuclease.[38–40] Methylpurine glycosylase also recognizes this lesion.[41–43] For instance, *E. coli* cells lacking the endo V (*nfi*) gene were shown to exhibit elevated mutation frequencies when exposed to nitrous acid. The increased mutations were predominantly A:T→G:C mutations, followed by lesser G:C→A:T mutations.[44,45] This indicates that endo V is primarily involved in the repair of dI lesions.[44–48]

The structure of double-stranded oligodeoxynucleotide containing the dI:dC pair was determined by thermodynamic and NMR studies.[49,50] dI can most stably pair with dC among four dNs, and its geometric structure is similar in form with the Watson–Crick structure (Fig. 8). dI has a carbonyl group at position C6 and a positive charge at position N1 after dA suffers from nitrosative deamination by ·NO. Thus, since the structure of dI is similar to that of dG rather than dA, the dI adduct can predominantly pair with dC, the wrong base.

In conclusion, nonradioactive kinetic studies and two-phased PAGE were performed to explore the

Table 2. $F_{ins} \times F_{ext}$ past DNA adducts by human DNA pol α, pol η, and pol κΔC

	Z=	dI[a]	dX[b]	8-NO_2-dG
Pol α	C:Z	**0.487**	4.50×10^{-4} [c]	1.69×10^{-3} [c]
	A:Z	N.D.	2.18×10^{-5} [c]	**1.31×10^{-5}** [c]
	G:Z	N.D.	1.11×10^{-5} [c]	2.63×10^{-6} [c]
	T:Z	2.32×10^{-4} [d]	**6.68×10^{-3}** [c]	5.87×10^{-6} [c]
Pol η	C:Z	**0.446**	5.24×10^{-2} [c]	6.94×10^{-4} [c]
	A:Z	1.16×10^{-4} [d]	1.71×10^{-3} [c]	**5.09×10^{-3}** [c]
	G:Z	6.86×10^{-5} [c]	2.93×10^{-4} [c]	4.63×10^{-4} [c]
	T:Z	1.39×10^{-3} [c]	**0.259**	4.06×10^{-4} [c]
Pol κΔC	C:Z	**0.642**	8.39×10^{-4} [c]	6.37×10^{-5} [c]
	A:Z	7.50×10^{-3} [c]	2.43×10^{-4} [c]	**2.88×10^{-4}** [c]
	G:Z	1.75×10^{-4} [c]	2.48×10^{-4} [c]	2.62×10^{-5} [c]
	T:Z	9.74×10^{-4} [d]	**5.12×10^{-2}** [c]	6.62×10^{-5} [c]

Values in boldface show a primarily misincorporated base opposite the DNA adduct.
N.D., not detectable.
[a] Data were taken from Table 1.
[b] Data were taken from Ref. 36.
[c] Data were taken from Ref. 34.

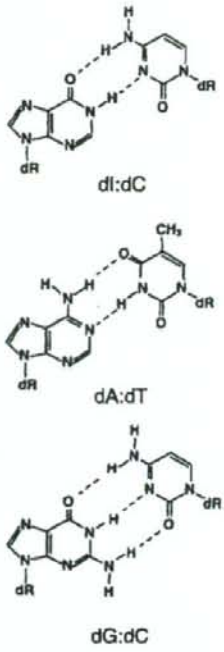

Fig. 8. Possible base pairing of the dI adduct with dC.

miscoding specificities and frequencies of the dI lesion catalyzed by Y-family human DNA pols. The dI adduct represents a highly miscoding lesion capable of generating A→G transitions, indicating that this $^{\bullet}NO$-induced lesion plays an important role in initiating inflammation-driven carcinogenesis.

Materials and Methods

General

Ultrapure dNTPs were from GE Healthcare. EcoRI restriction endonuclease (100 U/μL) was purchased from New England BioLabs. Blue Dextran (D5751) was obtained from Sigma. Human pol α was obtained from CHIMERx (Milwaukee, WI). Human pol η was purified as previously described.[19] Human pol κ (pol κΔC) was overexpressed in *E. coli* and purified as a C-terminally truncated form. The protein has 10× His tag at the N-terminal position and contains 559 amino acids from the N-terminus (N. Niimi and T. Nohmi *et al.*, unpublished results).

Preparation of oligodeoxynucleotides

All oligodeoxynucleotides, Alexa546 (Molecular Probes)-labeled primers, standard markers, and dI-modified template were obtained from Japan Bio Service Co. (Saitama, Japan). Alexa546 was conjugated at the 5'-terminus of primers and standard markers. A single dI was located at the 20th position from the 5'-termini in the modified 38-mer template (5'CATGCTGATGAATTCCTTCZCTTCTTTC-CTCTCCCTTT, where Z is dI). The oligomers were purified by using 20% denaturing PAGE before use.

Primer extension reactions

Primer extension reactions catalyzed by pol α, pol η, or pol κΔC were conducted at 25 °C for 30 min in a buffer (10 μL) containing all four dNTPs (100 μM each) using dI-modified and unmodified 38-mer templates (750 fmol) primed with an Alexa546-labeled 10-mer (500 fmol, 5' AGAGGAAAGA) (Fig. 3). The reaction buffer for pol α contains 40 mM Tris–HCl (pH 8.0), 5 mM $MgCl_2$, 60 mM KCl, 10 mM dithiothreitol, 250 μg/mL bovine serum albumin, and 2.5% glycerol. The reaction buffer for pol η and pol κΔC contains 40 mM Tris–HCl (pH 8.0), 1 mM $MgCl_2$, 10 mM dithiothreitol, 250 μg/mL bovine serum albumin, 60 mM KCl, and 2.5% glycerol. Reaction was stopped by addition of 2 μL formamide dye containing Blue Dextran (100 mg/mL) and ethylenediaminetetraacetic acid (50 mM) and incubation at 95 °C for 3 min. The whole amount of the reaction sample was subjected to 20% denaturing PAGE (30 × 40 × 0.05 cm). The positions of bands and homogeneities of oligodeoxynucleotides following PAGE were determined by using Molecular Imager FX Pro and Quantity One software (Bio-Rad). The linear range to quantitatively detect fluorescence-labeled oligomers was from 5 to 1500 fmol (Fig. 6).

Quantitation of miscoding specificity

Using dI-modified and unmodified 38-mer oligodeoxynucleotide (750 fmol) primed with an Alexa546-labeled 12-mer (500 fmol, 5'AGAGGAAAGAAG), we conducted primer extension reactions catalyzed by pol α (200 fmol), pol η (20 fmol), or pol κΔC (20 fmol) at 25 °C for 30 min in a buffer (10 μL) containing all four dNTPs (100 μM each) and subjected them to 20% denaturing PAGE (30 × 40 × 0.05 cm). Extended reaction products (>26 bases long) were extracted from the gel. The recovered oligodeoxynucleotides were annealed with an unmodified 38-mer, cleaved with EcoRI, and subjected to two-phased PAGE (20 × 65 × 0.05 cm) containing 7 M urea in the upper phase and no urea in the middle and bottom phases (each phase contains 18%, 20%, and 24% polyacrylamide, respectively). The phase width is approximately 10, 37, and 18 cm from the upper phase. To quantify base substitutions and deletions, we compared the mobility of the reaction products with those of Alexa546-labeled 18-mer standards containing dC, dA, dG, or dT opposite the lesion and one-base (Δ^1) or two-base (Δ^2) deletions[17,18] (Fig. 3).

Steady-state kinetic studies of nucleotide insertion and extension

Kinetic parameters associated with nucleotide insertion opposite the dI lesion and chain extension from the 3' primer terminus were determined at 25 °C, using varying amounts of single dNTPs. For insertion kinetics, reaction mixtures containing dNTP (0–250 μM) and either pol α (20–200 fmol), pol η (2–20 fmol), or pol κΔC (1–20 fmol) were incubated at 25 °C for 2 min in 10 μL of Tris–HCl buffer (pH 8.0) using a 38-mer template (750 fmol) primed with an Alexa546-labeled 12-mer (500 fmol; 5'AGAG-

GAAAGAAG). Reaction mixtures containing a 38-mer template (750 fmol) primed with an Alexa546-labeled 13-mer (500 fmol; 5'AGAGGAAAGAAGN, where N is C, A, G, or T), with varying amounts of dGTP (0–250 μM) and either pol η (20–200 fmol), pol η (1–20 fmol), or pol η ΔC (1–20 fmol), were used to measure chain extension. The reaction samples were subjected to 20% denaturing PAGE (30 × 40 × 0.05 cm). The Michaelis constants (K_m) and maximum rates of reaction (V_{max}) were obtained from Hanes–Woolf plots. Frequencies of dNTP insertion (F_{ins}) and chain extension (F_{ext}) were determined relative to the dT:dA base pair according to the following equation: $F = (V_{max}/K_m)_{[wrong\ pair]}/(V_{max}/K_m)_{[correct\ pair\ with\ dT:dA]}$.[24,25]

Acknowledgements

This research was supported in part by Grants-in-aid for Scientific Research 19710059 from the Ministry of Education, Culture, Sports, Science and Technology (to M.Y.). This work was also partially supported by Health, Welfare, and Labor Science Research Grants (H18-food-general-009) and a Grant-in-aid (KHB1007) from the Japan Health Science Foundation (to M.H.).

References

1. Ohshima, H. & Bartsch, H. (1994). Chronic infections and inflammatory processes as cancer risk factors: possible role of nitric oxide in carcinogenesis. *Mutat. Res.* **305**, 253–264.
2. Cassell, G. H. (1998). Infectious causes of chronic inflammatory diseases and cancer. *Emerg. Infect. Dis.* **4**, 475–487.
3. Ohshima, H., Tatemichi, M. & Sawa, T. (2003). Chemical basis of inflammation-induced carcinogenesis. *Arch. Biochem. Biophys.* **417**, 3–11.
4. Burney, S., Caulfield, J. L., Niles, J. C., Wishnok, J. S. & Tannenbaum, S. R. (1999). The chemistry of DNA damage from nitric oxide and peroxynitrite. *Mutat. Res.* **424**, 37–49.
5. deRojas-Walker, T., Tamir, S., Ji, H., Wishnok, J. S. & Tannenbaum, S. R. (1995). Nitric oxide induces oxidative damage in addition to deamination in macrophage DNA. *Chem. Res. Toxicol.* **8**, 473–477.
6. Yermilov, V., Rubio, J., Becchi, M., Friesen, M. D., Pignatelli, B. & Ohshima, H. (1995). Formation of 8-nitroguanine by the reaction of guanine with peroxynitrite *in vitro*. *Carcinogenesis*, **16**, 2045–2050.
7. Yermilov, V., Rubio, J. & Ohshima, H. (1995). Formation of 8-nitroguanine in DNA treated with peroxynitrite *in vitro* and its rapid removal from DNA by depurination. *FEBS Lett.* **376**, 207–210.
8. Lewis, R. S., Tannenbaum, S. R. & Deen, W. M. (1995). Kinetics of N-nitrosation in oxygenated nitric oxide solutions at physiological pH: role of nitrous anhydride and effects of phosphate and chloride. *J. Am. Chem. Soc.* **117**, 3933–3939.
9. Wink, D. A., Kasprzak, K. S., Maragos, C. M., Elespuru, R. K., Misra, M., Dunams, T. M. *et al.* (1991). DNA deaminating ability and genotoxicity of nitric oxide and its progenitors. *Science*, **254**, 1001–1003.
10. Nguyen, T., Brunson, D., Crespi, C. L., Penman, B. W., Wishnok, J. S. & Tannenbaum, S. R. (1992). DNA damage and mutation in human cells exposed to nitric oxide *in vitro*. *Proc. Natl Acad. Sci. USA*, **89**, 3030–3034.
11. Caulfield, J. L., Wishnok, J. S. & Tannenbaum, S. R. (1998). Nitric oxide-induced deamination of cytosine and guanine in deoxynucleosides and oligonucleotides. *J. Biol. Chem.* **273**, 12689–12695.
12. Dong, M., Wang, C., Deen, W. M. & Dedon, P. C. (2003). Absence of 2'-deoxyoxanosine and presence of abasic sites in DNA exposed to nitric oxide at controlled physiological concentrations. *Chem. Res. Toxicol.* **16**, 1044–1055.
13. Pang, B., Zhou, X., Yu, H., Dong, M., Taghizadeh, K., Wishnok, J. S. *et al.* (2007). Lipid peroxidation dominates the chemistry of DNA adduct formation in a mouse model of inflammation. *Carcinogenesis*, **28**, 1807–1813.
14. Dong, M. & Dedon, P. C. (2006). Relatively small increases in the steady-state levels of nucleobase deamination products in DNA from human TK6 cells exposed to toxic levels of nitric oxide. *Chem. Res. Toxicol.* **19**, 50–57.
15. Gal, A. & Wogan, G. N. (1996). Mutagenesis associated with nitric oxide production in transgenic Sfl. mice. *Proc. Natl Acad. Sci. USA*, **93**, 15102–15107.
16. Kamiya, H., Sakaguchi, T., Murata, N., Fujimuro, M., Miura, H., Ishikawa, H. *et al.* (1992). *In vitro* replication study of modified bases in ras sequences. *Chem. Pharm. Bull.* **40**, 2792–2795.
17. Masutani, C., Araki, M., Yamada, A., Kusumoto, R., Nogimori, T., Maekawa, T. *et al.* (1999). Xeroderma pigmentosum variant (XP-V) correcting protein from HeLa cells has a thymine dimer bypass DNA polymerase activity. *EMBO J.* **18**, 3491–3501.
18. Ogi, T., Kato, T., Jr, Kato, T. & Ohmori, H. (1999). Mutation enhancement by DINB1, a mammalian homologue of the *Escherichia coli* mutagenesis protein dinB. *Genes Cells*, **4**, 607–618.
19. Gerlach, V. L., Aravind, L., Gotway, G., Schultz, R. A., Koonin, E. V. & Friedberg, E. C. (1999). Human and mouse homologs of *Escherichia coli* DinB (DNA polymerase IV), members of the UmuC/DinB superfamily. *Proc. Natl Acad. Sci. USA*, **96**, 11922–11927.
20. Goodman, M. F. & Tippen, B. (2000). The expanding polymerase universe. *Nat. Rev., Mol. Cell Biol.* **1**, 101–109.
21. Kunkel, T. A., Pavlov, Y. I. & Bebenek, K. (2003). Functions of human DNA polymerases η, κ and ι suggested by their properties, including fidelity with undamaged DNA templates. *DNA Repair*, **3**, 135–149.
22. Shibutani, S. (1993). Quantitation of base substitutions and deletions induced by chemical mutagens during DNA synthesis *in vitro*. *Chem. Res. Toxicol.* **6**, 625–629.
23. Shibutani, S., Suzuki, N., Matsumoto, Y. & Grollman, A. P. (1996). Miscoding properties of $3,N^4$-etheno-2'-deoxycytidine in reactions catalyzed by mammalian DNA polymerases. *Biochemistry*, **35**, 14992–14998.
24. Mendelman, L. V., Boosalis, M. S., Petruska, J. & Goodman, M. F. (1989). Nearest neighbor influences on DNA polymerase insertion fidelity. *J. Biol. Chem.* **264**, 14415–14423.
25. Mendelman, L. V., Petruska, J. & Goodman, M. F. (1990). Base mispair extension kinetics. Comparison of DNA polymerase alpha and reverse transcriptase. *J. Biol. Chem.* **265**, 2338–2346.
26. Clark, J. M., Joyce, C. M. & Beardsley, G. P. (1987). Novel blunt-end addition reactions catalyzed by DNA polymerase I of *Escherichia coli*. *J. Mol. Biol.* **198**, 123–127.

27. Terashima, I., Suzuki, N., Dasaradhi, L., Tan, C.-K., Downey, K. M. & Shibutani, S. (1998). Translesional synthesis on DNA templates containing an estrogen quinone derived adduct: N^2-(2-hydroxyestron-6-yl)-2'-deoxyguonosine and N^6-(2-hydroxyestron-6-yl)-2'-deoxyadenosine. *Biochemistry*, **37**, 13807–13815.
28. Routledge, M. N., Wink, D. A., Keefer, L. K. & Dipple, A. (1993). Mutations induced by saturated aqueous nitric oxide in the pSP189 *supF* gene in human Ad293 and *E. coli* MBM7070 cells. *Carcinogenesis*, **14**, 1251–1254.
29. Kelman, D. J., Christodolou, D., Wink, D. A., Keefer, L. K., Srinivasan, A. & Dipple, A. (1997). Relative mutagenicities of gaseous nitrogen oxides in the *supF* gene of pSP189. *Carcinogenesis*, **18**, 1045–1048.
30. Routledge, M. N., Wink, D. A., Keefer, L. K. & Dipple, A. (1994). DNA sequence changes induced by two nitric oxide donor drugs in the *supF* assay. *Chem. Res. Toxicol.* **7**, 628–632.
31. Juedes, M. J. & Wogan, G. N. (1996). Peroxynitrite-induced mutation spectra of pSP189 following replication in bacteria and in human cells. *Mutat. Res.* **349**, 51–61.
32. Kim, M. Y., Dong, M., Dedon, P. C. & Wogan, G. N. (2005). Effects of peroxynitrite dose and dose rate on DNA damage and mutation in the *supF* shuttle vector. *Chem. Res. Toxicol.* **18**, 76–86.
33. Routledge, M. N. (2000). Mutations induced by reactive nitrogen oxide species in the *supF* forward mutation assay. *Mutat. Res.* **450**, 95–105.
34. Suzuki, N., Yasui, M., Geacintov, N. E., Shafirovich, V. & Shibutani, S. (2005). Miscoding events during DNA synthesis past the nitration-damaged base 8-nitroguanine. *Biochemistry*, **44**, 9238–9245.
35. Shibutani, S., Takeshita, M. & Grollman, A. P. (1991). Insertion of specific bases during DNA synthesis past the oxidation-damaged base 8-oxodG. *Nature*, **349**, 431–434.
36. Yasui, M., Suzuki, N., Miller, H., Matsuda, T., Matsui, S. & Shibutani, S. (2004). Translesion synthesis past 2'-deoxyxanthosine, a nitric oxide-derived DNA adduct, by mammalian DNA polymerases. *J. Mol Biol.* **344**, 665–674.
37. Kamiya, H., Miura, H., Kato, H., Nishimura, S. & Ohtsuka, E. (1992). Induction of mutation of a synthetic c-Ha-*ras* gene containing hypoxanthine. *Cancer Res.* **52**, 1836–1839.
38. Yao, M. & Kow, Y. W. (1996). Cleavage of insertion/deletion mismatches, flap and pseudo-Y DNA structures by deoxyinosine 3'-endonuclease from *Escherichia coli*. *J. Biol. Chem.* **271**, 30672–30676.
39. Yao, M., Hatahet, Z., Melamede, R. J. & Kow, Y. W. (1994). Purification and characterization of a novel deoxyinosine-specific enzyme, deoxyinosine 3' endonuclease, from *Escherichia coli*. *J. Biol. Chem.* **269**, 16260–16268.
40. Yao, M. & Kow, Y. W. (1995). Interaction of deoxyinosine 3'-endonuclease from *Escherichia coli* with DNA containing deoxyinosine. *J. Biol. Chem.* **270**, 28609–28616.
41. Saparbaev, M. & Laval, J. (1994). Excision of hypoxanthine from DNA containing dIMP residues by the *Escherichia coli*, yeast, rat, and human alkylpurine DNA glycosylases. *Proc. Natl Acad. Sci. USA*, **91**, 5873–5877.
42. Fortini, P., Parlanti, E., Sidorkina, O. M., Laval, J. & Dogliotti, E. (1999). The type of DNA glycosylase determines the base excision repair pathway in mammalian cells. *J. Biol. Chem.* **274**, 15230–15236.
43. Miao, F., Bouziane, M. & O'Connor, T. R. (1998). Interaction of the recombinant human methylpurine-DNA glycosylase (MPG protein) with oligodeoxyribonucleotides containing either hypoxanthine or abasic sites. *Nucleic Acids Res.* **26**, 4034–4041.
44. Schouten, K. A. & Weiss, B. (1999). Endonuclease V protects *Escherichia coli* against specific mutations caused by nitrous acid. *Mutat. Res.* **435**, 245–254.
45. Weiss, B. (2006). Evidence for mutagenesis by nitric oxide during nitrate metabolism in *Escherichia coli*. *J. Bacteriol.* **188**, 829–833.
46. Guo, G. & Weiss, B. (1998). Endonuclease V (*nfi*) mutant of *Escherichia coli* K-12. *J. Bacteriol.* **180**, 46–51.
47. Dong, M., Vongchampa, V., Gingipalli, L., Cloutier, J. F., Kow, Y. W., O'Connor, T. & Dedon, P. C. (2006). Development of enzymatic probes of oxidative and nitrosative DNA damage caused by reactive nitrogen species. *Mutat. Res.* **594**, 120–134.
48. Weiss, B. (2001). Endonuclease V of *Escherichia coli* prevents mutations from nitrosative deamination during nitrate/nitrite respiration. *Mutat. Res.* **461**, 301–309.
49. Kawase, Y., Iwai, S., Inoue, H., Miura, K. & Ohtsuka, E. (1986). Studies on nucleic acid interactions. I. Stabilities of mini-duplexes (dG2A4XA4G2–dC2T4YT4C2) and self-complementary d(GGGAAXYTTCCC) containing deoxyinosine and other mismatched bases. *Nucleic Acids Res.* **14**, 7727–7736.
50. Uesugi, S., Oda, Y., Ikehara, M., Kawase, Y. & Ohtsuka, E. (1987). Identification of I:A mismatch base-pairing structure in DNA. *J. Biol. Chem.* **262**, 6965–6968.

Radiat Environ Biophys (2008) 47:439–444
DOI 10.1007/s00411-008-0179-7

ORIGINAL PAPER

Repair of I-SceI Induced DSB at a specific site of chromosome in human cells: influence of low-dose, low-dose-rate gamma-rays

Fumio Yatagai · Masao Suzuki · Noriaki Ishioka · Hitoshi Ohmori · Masamitsu Honma

Received: 9 January 2008 / Accepted: 5 June 2008 / Published online: 21 June 2008

Abstract We investigated the influence of low-dose, low-dose-rate gamma-ray irradiation on DNA double strand break (DSB) repair in human lymphoblastoid TK6 cells. A single DSB was introduced at intron 4 of the *TK*+ allele (chromosome 17) by transfection with the I-SceI expression vector pCBASce. We assessed for DSB repair due to non-homologous end-joining (NHEJ) by determining the generation of TK-deficient mutants in the TK6 derivative TSCE5 (*TK* +/−) carrying an I-SceI recognition site. We similarly estimated DSB repair via homologous recombination (HR) at the same site in the derived compound heterozygote (*TK*−/−) cell line TSCER2 that carries an additional point mutation in exon 5. The NHEJ repair of DSB was barely influenced by pre-irradiation of the cells with 30 mGy γ-rays at 1.2 mGy h^{-1}. DSB repair by HR, in contrast, was enhanced by ~50% after pre-irradiation of the cells under these conditions. Furthermore, when I-SceI digestion was followed by irradiation at a dose of 8.5 mGy, delivered at a dose rate of only 0.125 mGy h^{-1}, HR repair efficiency was enhanced by ~80%. This experimental approach can be applied to characterize DSB repair in the low-dose region of ionizing radiation.

F. Yatagai (✉) · H. Ohmori
Advanced Development and Support Center,
The Institute of Physical and Chemical Research (RIKEN),
Saitama 351-0198, Japan
e-mail: yatagai@postman.riken.go.jp

M. Suzuki
Heavy-ion Medical Science Center,
National Institute of Radiological Sciences,
Chiba-shi, Chiba, Japan

N. Ishioka
Japan Aerospace Exploration Agency,
Institute of Space and Astronautical Science,
Tsukuba-shi, Ibaraki, Japan

M. Honma
Division of Genetics and Mutagenesis,
National Institute of Health Sciences, Tokyo, Japan

Introduction

Health risks from low doses of ionizing radiation (IR) are of concern and it is important to estimate such risks for persons occupationally exposed to IR, such as airline crews, astronauts, and some workers in medical and industrial fields, including those in nuclear plants. Genetic analyses for induction of mutations, chromosome aberrations, micronuclei etc., are frequently used to estimate radiation risk. A new sensitive methodology developed in Honma's laboratory—analysis of loss of heterozygosity (LOH) at the *thymidine kinase* (*TK*) locus in human lymphoblastoid TK6 cells [1, 2]—can detect LOH events (interstitial deletions) in cells exposed to low doses of γ-rays delivered at a low dose rate, such as 30 mGy delivered at 1.2 mGy h^{-1} [3]. The LOH events are most likely a consequence of inaccurate repair of DNA double-strand breaks (DSBs), the most dangerous DNA lesion induced by IR. The high frequency of interstitial deletions observed after a low dose (30 mGy) exposure was unexpected because the estimated probability of generating two DSBs in the *TK* locus region is low under these conditions ($<2.25 \times 10^{-10}$) [3]. Thus, the radiation-induced DSBs seem unlikely to initiate the interstitial deletions. Rather, the deletions might result from IR interfering with correct repair of spontaneous DSBs or from the conversion of other damage, such as single-strand breaks.

When we tried to explore the influence of low-dose IR on DSB repair, we found it difficult to track specifically DSBs

amid the variety of DNA lesions that were induced. We therefore constructed a model system that could trace the fate of a single DSB [4, 5]. Our system can distinguish two major DSB repair pathways, non-homologous end-joining (NHEJ) and homologous recombination (HR) [6, 7]. NHEJ joins broken ends, which have little or no sequence homology in a non-conservative manner, and some information may be lost in the course of the repair process. HR, on the other hand, requires extensive tracts of sequence homology and is generally considered as error-free [8].

The human cell line TSCE5 is heterozygous (+/−) for the *TK* gene and the line TSCER2 is compound heterozygous (−/−); both carry an I-SceI endonuclease recognition site in intron 4 of one allele of the *TK* gene. DSBs can be generated at the I-SceI site by expression of the I-SceI vector [4]. When DSBs occur at the *TK* locus, NHEJ in TSCE5 cells produces TK-deficient mutants while HR between the *TK* alleles in TSCER2 cells produces TK-proficient revertants. This means that positive–negative drug selection for TK phenotypes permits distinction between NHEJ and HR repair.

The LOH analysis of TK mutants suggests that low-dose, low-dose-rate IR has important indirect effects. When the I-SceI model system is applied to estimating the influence of low-level IR on repair of a specifically introduced DSB, we can estimate the indirect effects of the exposure because the IR-damaged site can be ignored as a repair target. Here, we first examined whether such indirect effect can be detected by an experiment based upon the original concept of radioadaptation, a priming exposure to low-dose, low-dose-rate IR followed by the challenging treatment of I-SceI digestion. Second, a new type of experiment, the I-SceI treatment followed by low-dose, low-dose-rate IR exposure, was performed to investigate certain kinds of indirect effect, such as an influence of high radiation background exposure on DSB repair, because the continuous expression of I-SceI vector after the cell transfection mimics the above situation. These experiments provided the interesting finding that low level IR enhances the HR pathway.

Materials and methods

Cell line construction

Figure 1 outlines the structure of the repair substrates and the cell lines; the details of the strain construction were described previously [4]. Briefly, in lymphoblastoid TK6 cells heterozygous for the TK gene, the functional allele was first inactivated by gene targeting with vector pTK4 to replace exon 5 of the *TK* gene by a *neo* gene. To introduce the I-SceI recognition site, in a second step the targeting vector, pTK10, encompassing about 6 kb of the original *TK* gene with exons 5, 6, and 7, and the I-SceI recognition site in intron 4, 75 bp upstream of exon 5, was used to revert the *TK* gene disrupted by pTK4. The new line was termed TSCE5. A spontaneous reversion in a TSCE5 cell (G to A in position 23 of exon 5), which we cloned, led to the compound heterozygote (*TK*−/−) cell line, TSCER2. In TSCE5, when a DSB at the I-SceI site is repaired by NHEJ involving a deletion in the adjacent exon, the cell can be isolated as a TK-deficient mutant. In TSCER2, when a DSB is repaired by HR between the *TK* alleles, a TK^{+} allele can be generated, resulting in a revertant phenotype.

Cell culture and IR exposure

Cell culture details were described in earlier work [1–3]. We tested the response of TSCE5 and TSCER2 cells cultured in RPMI1640 medium to low-dose, low-dose-rate γ-irradiation in a 5% CO_2 incubator both before (mode A, Fig. 2) and after (mode B, Fig. 2) I-SceI digestion. In mode A, the cells were exposed to ^{60}Co γ-rays at 1.2 mGy h^{-1} for 25 h (total exposure, 30 mGy) and reached a cell concentration of 8×10^5 ml^{-1} at the end of the irradiation/culture period. Then, 2 h after finishing the γ-irradiation, the cells were transfected with the I-SceI expression vector. The delay occurred because the radiation exposure facility was located far from the biological experimental area. In mode B, the cells were transfected with the vector first and 2 h later exposed to a much lower γ-ray dose and dose-rate (~28% of the mode A dose at ~10% of the mode A dose rate), namely 0.125 mGy h^{-1} for 68 h (total exposure, 8.5 mGy). In an independent determination performed with 8 cell culture flasks in duplicate experiments, cells were exposed for 96 h (total exposure, 12 mGy). At the end of irradiation/culture period in mode B, the cell concentration was adjusted to 8×10^5 ml^{-1}. Control cells were treated in the same manner except that they were not irradiated. The γ-irradiations were performed at the National Institute of Radiological Studies (NIRS), and the adjustment of dose-rate was done by changing the distance between the ^{60}Co source and the CO_2 incubator.

I-SceI expression

We introduced the I-SceI expression vector (pCBASce) by suspending 5×10^6 cells in 0.1 ml Nucleofector Solution V (amaxa AG, Cologne, Germany) with 50 μg of uncut pCBSce vector, or without the vector as a control, following the manufacturer's recommendations [5]. Although we could not determine the efficiency of DSB generation under the present condition of transfection, the I-SceI expression vector was introduced into about 65% of the cells at 24 h after the transfection and the expression lasts for 3 days incubation [5].